reported that background prevents, or makes difficult, the acquisition of quality Raman data. For example, Stencel et al.[14] recently reported that difficulties in obtaining spectra were encountered due to an intense fluorescence background for Mo-SiO_2 catalysts with loadings of Mo below 5%. In this case, however, the chemical structure responsible for fluorescence was not identified.

Transition-metal ion (particularly Fe^{3+}) impurities,[15] color centers and crystal defects,[15,16] and surface and bulk excitons[17] have been discussed as possible origins of the scattering background. Careri et al.[18] related the scattering background to the presence of water molecules tightly hydrogen bonded close to Lewis acid sites and showed the intensity of the scattering background was strongly dependent on the nature of the oxide. Jeziorowski and Knozinger[19] showed that surface hydroxide ions were responsible for the so-called "fluorescence" background for MgO and Al_2O_3. These latter authors obtain a clear correlation between background intensity and hydroxyl group density of the MgO surface. For alumina, the latter authors detected two distinct hydroxyl groups which they tentatively attributed to terminal -OH groups coordinated to a tetrahedral or an octahedral cation, respectively. In light of the observations of Jeziorowski and Knozinger, it appears likely that the intense background for the higher Hf containing materials is due to hydroxyls or water. If this is the case then either (1) the Hf would have to retain water or hydroxyls much more strongly than Zr or (2) the hydroxyls associated with Hf, but not those with Zr, are responsible for the background. However, either of these two cases would be surprising.

The Raman data and the surface characterization data in ref 8 are consistent with a surface Hf composition that is very close to that of the bulk. From the similarity of the surface analysis and Raman data for the surface impregnated and bulk samples, it is concluded that the Hf added to the surface by impregnation of the calcined zirconia remains on the surface even following calcination at 600 °C. Upon heating to 1000 °C, the surface Hf becomes mobile and diffuses into the bulk.

The surface characterization data therefore indicate that the surface fraction of Hf is essentially equal to the bulk fraction for coprecipitated catalysts. Furthermore, the impregnated sample retained the Hf on the surface to provide the composition prepared by impregnation. In this respect it appears that the hafnium oxide-zirconium oxide system provides an excellent catalyst system for evaluating the importance of surface or bulk factors in determining catalytic properties. However, the selectivity for alcohol dehydration, while interesting in itself, appears to be too complex to be used for this purpose.

Acknowledgment. This work was supported, in part, by the Kentucky Energy Cabinet Laboratory (KECL) with funding from the Commonwealth of Kentucky, Kentucky Energy Cabinet. The KECL is administered under contract by the University of Louisville.

Registry No. HfO_2, 12055-23-1; ZrO_2, 1314-23-4.

(14) Stencel, J. M.; Diehl, J. R.; D'Este, J. R.; Makovsky, L. E.; Rodrigo, L.; Marcinkowska, K.; Adnot, A.; Roberge, P. C.; Kaliaguine, S. *J. Phys. Chem.* **1986**, *90*, 4739.
(15) Egerton, T. A.; Hardin, A. H.; Kozirovski, Y.; Sheppard, N. *J. Catal.* **1974**, *32*, 343.
(16) Angel, C. L. *J. Phys. Chem.* **1973**, *77*, 222.
(17) Jeziorowski, H.; Knozinger, H. *Chem. Phys. Lett.* **1976**, *42*, 162.
(18) Careri, G.; Mazzacurati, V.; Sampoli, M.; Signorelli, G. *J. Catal.* **1972**, *26*, 494.
(19) Jeziorowski, H.; Knozinger, H. *Chem. Phys. Lett.* **1977**, *51*, 519.

Second Harmonic Generation Studies of Hydrogen Evolution from Polycrystalline Silver Electrodes in Acetonitrile

Deborah J. Campbell and Robert M. Corn*

Department of Chemistry, University of Wisconsin—Madison, Madison, Wisconsin 53706
(Received: March 16, 1987)

The optical second harmonic generation from polycrystalline silver electrodes decreases in a reversible manner during the evolution of molecular hydrogen in acetonitrile solutions containing a variety of acids. The observed changes are ascribed to the modification of the nonlinear response of the electrons at the metal surface by the adsorption of a monatomic hydrogen species. The relative surface coverage of adsorbed hydrogen as a function of potential and of acid strength can be calculated from the optical data; a comparison of the calculated surface coverages with those predicted from various models reveals the reaction mechanism for the formation of molecular hydrogen. The hydrogen evolution reaction on silver electrodes in acetonitrile proceeds via a two-step process: an initial ion-discharge reaction which creates an adsorbed monatomic hydrogen species on the surface, followed by a biatomic surface combination reaction.

Introduction

The nonlinear process of optical second harmonic generation (SHG) is inherently sensitive to the interface of two centrosymmetric media. This sensitivity arises from the relaxation of the bulk symmetry at the interface (SHG is an electric dipole forbidden process in centrosymmetric media)[1] and has led to a significant increase in the interest and use of SHG as a spectroscopic probe of surfaces.[2] In particular, SHG has been used extensively as an in situ measurement on polycrystalline and single-crystal silver electrodes.[3-11] A number of SHG studies have measured

(1) Bloembergen, N.; Chang, R. K.; Jha, S. S.; Lee, C. H. *Phys. Rev.* **1968**, *174*, 813.
(2) For example, see (a) Shen, Y. R. *The Principles of Nonlinear Optics*; Wiley: New York, 1984. (b) *Chem. Eng. News.* **64** (Oct 6), 22.
(3) (a) Chen, C. K.; Heinz, T. F.; Ricard, D.; Shen, Y. R. *Phys. Rev. Lett.* **1981**, *46*, 1010. (b) Heinz, T. F.; Chen, C. K.; Ricard, D.; Shen, Y. R. *Chem. Phys. Lett.* **83**, **1983**, 180.
(4) Murphy, D. V.; von Raben, K. U.; Chen, T. T.; Owen, J. F.; Chang, R. K.; Laube, B. L. *Surf. Sci.* **1983**, *124*, 529.
(5) Corn, R. M.; Romagnoli, M.; Levenson, M. D.; Philpott, M. R. *Chem. Phys. Lett.* **1984**, *106*, 30.
(6) Corn, R. M.; Romagnoli, M.; Levenson, M. D.; Philpott, M. R. *J. Chem. Phys.* **1984**, *81*, 4127.
(7) (a) Richmond, G. L. *Chem. Phys. Lett.* **1984**, *106*, 26. (b) Richmond, G. L. *Langmuir* **1986**, *2*, 132, and references therein.
(8) Richmond, G. L. *Chem. Phys. Lett.* **1985**, *110*, 571.

0022-3654/87/2091-5668$01.50/0

the electromagnetic field enhancements that occur at silver surfaces which have undergone some type of roughening procedure;[3,4] more recent efforts[5-11] have demonstrated that the SHG signal can be used to monitor surface properties even in the absence of significant roughening.

In our previous studies of vacuum-deposited thin film silver electrodes, we examined the SHG signal created via surface polaritons.[5,6] The SHG signal from the interface was found to arise primarily from the optical response of the metal electrons at the electrode surface; a simple model relating the excess charge density to the SHG intensity (hereafter referred to as the "charge-induced SHG mechanism") sufficiently explained these and other results.[8] Further studies by a number of groups have subsequently demonstrated, however, that the charge-induced SHG mechanism cannot describe all of the SHG experiments: changes upon the underpotential deposition of Pb and Tl monolayers,[6,11] and upon a slight surface oxidation[9] were found to alter the nonlinear optical response of the metal surface significantly.

To date, all of the SHG studies on silver electrodes have been undertaken in aqueous electrochemical systems, where the evolution of molecular hydrogen from water normally limits the available potential window to about 1.5 V. This limitation can be surmounted by employing a nonaqueous solvent such as acetonitrile, which greatly extends the available potential range and enables the study of water-sensitive compounds.[12] However, differential capacitance studies in acetonitrile indicate that the adsorption of solvent molecules to the electrode surface changes the nature of the electrochemical interface and strongly inhibits the adsorption of electroactive species.[13] For example, the hydrogen evolution reaction on platinum electrodes is inhibited and electrochemically irreversible in acetonitrile,[14] as compared to the electrochemically reversible adsorption of hydrogen atoms on platinum which occurs during hydrogen evolution in aqueous acid solutions.[15] The adsorption of acetonitrile is expected to occur on silver electrodes as well.[16] A number of the previous electrochemical SHG studies have shown that the SHG signal can be sensitive to pH[7] and molecular and ionic adsorption,[3,8,10] although in some cases[10] it is unclear whether the observed changes in the SHG signal arise from alterations in the optical response of the metal surface, or from the inherent nonlinear susceptibility of the molecules.

To further elucidate the effect of adsorption on SHG from electrochemical surfaces, and to demonstrate the utility of SHG in nonaqueous electrochemical systems, we present here the results from a number of experiments in which we monitored the SHG signal from polycrystalline silver electrodes in acetonitrile solutions containing small (millimolar) quantities of various acids. The SHG signal from the surface is found to decrease during the highly irreversible process of molecular hydrogen evolution. The magnitude of this decrease is a function of the electrode potential and is independent of scan rate or direction. The changes in the SHG signal during this faradaic process can be ascribed to the adsorption of a monatomic hydrogen species prior to the formation of molecular hydrogen. Since it is unlikely that the adsorbed hydrogen moiety contributes to the surface nonlinear susceptibility, the observed modifications in the SHG signal must result from changes in the optical response of the electrons at the metal surface. These changes occur either through a decrease in the surface free electron density, or through an increase in the scattering of free electrons at the interface.[17]

From the SHG signal we can calculate the relative surface coverage of adsorbed hydrogen as a function of the applied potential and the hydrogen ion activity. By assuming that at each potential we are measuring the steady-state relative surface coverage of adsorbed hydrogen, we can compare the experimental results with the calculations of the relative surface coverage from a number of possible reaction mechanisms. We find that the only reaction mechanism which correctly predicts the potential and hydrogen ion activity dependence of the SHG signal in the series of acids studied is one in which the creation of molecular hydrogen proceeds by a two-step process: the formation of adsorbed monatomic hydrogen by the irreversible electrochemical reaction of hydrogen ions at the surface, followed by a surface combination reaction of two adsorbed hydrogen atom species.

Experimental Considerations

The SHG experiments employed the 15-ns pulses of 1064-nm light from a Quantel Model 580 Nd:YAG laser at a 10-Hz repetition rate and were run in an external reflection geometry with a 31° angle of incidence (after accounting for the changes in the optical path through the cell window). The 532-nm light generated at the electrode surface was separated from the fundamental beam by a narrow-band interference filter and subsequently detected and analyzed with a Hamamatsu Model R1477 photomultiplier tube and a Stanford Research SR-250 boxcar averager. The observed current pulses corresponded to between roughly 5 and 500 photoelectrons per shot for laser powers between 2 and 6 mJ per pulse. These numbers are lower than those which we observed on silver electrodes in aqueous electrochemical systems. To minimize the possibility of damaging the surface through absorptive heating, the laser power on the sample was kept at a minimum and the SHG signal averaged over a number of forward and reverse scans whenever the SHG intensity was found to be reversible (independent of scan direction). All of the SHG-potential curves presented in this paper are such averages.

UV grade acetonitrile was obtained from Burdick-Jackson and cleaned by passing over activated alumina (Universal Scientific Inc.) just prior to use. The acetonitrile solutions contained either $LiClO_4$ (GFS Chemical) or tetrabutylammonium tetrafluoroborate (Southwestern Analytical Chemicals Inc.) that had been twice recrystallized and vacuum-dried. The electrochemical cell was controlled by a Princeton Applied Research 173/175 potentiostat/pulse programmer in the standard three-electrode configuration: platinum counter electrode, silver working electrode, and a Ag|0.100 M $AgNO_3$ reference electrode. All potentials reported here are vs. Ag/Ag^+. The silver working electrode was a 7-mm-diameter "Puratronic grade" silver rod (Aesar) that was press fit into a Telfon rod, polished with alumina, and then sonicated prior to use. The Teflon rod was then inserted into a cell constructed from Kel-F with a single optical window of BK7 glass. The electrochemical scans revealed an unavoidable trace amount of water in the electrolyte with an estimated concentration of less than 1 mM. A small amount of residual polishing alumina was also observed in the first electrochemical scan, after which no traces could be found. The current, the potential, and SHG signal (i.e., the output of the boxcar averager) were all collected and stored in real time with an A/D converter and an IBM PC.

Results and Discussion

SHG-Potential Curves and Cyclic Voltammograms from Acetonitrile Solutions. The current and the SHG signal obtained from a polycrystalline silver electrode during the cycling of the electrode potential while in contact with an acetonitrile solution containing 0.1 M tetrabutylammonium tetrafluoroborate are plotted in Figure 1. The current waveform exhibits a small peak (ca. 30 $\mu A/cm^2$) at −1.18 V due to the breakdown of the residual water in the solution.[12] The average SHG signal from these background scans is a slowly varying function of potential. In some solutions (depending on the electrolyte and the amount of residual water), a slight break in the SHG signal was observed

(9) Richmond, G. L. *Chem. Phys. Lett.* **1985**, *113*, 359.
(10) Voss, D. F.; Nagumo, M.; Goldberg, L. S.; Bunding, K. A. *J. Phys. Chem.* **1986**, *90*, 1834.
(11) Furtak, T. E.; Miragliotta, J.; Korenowski, G. M., preprint.
(12) Billon, J. P. *J. Electroanal. Chem.* **1960**, *1*, 486.
(13) Petrii, D. A.; Khomchenko, I. G. *J. Electroanal. Chem.* **1980**, *106*, 277.
(14) Angerstein-Kozlowska, H.; MacDougall, B.; Conway, B. E. *J. Electroanal. Chem.* **1972**, *39*, 287.
(15) Woodard, F. E.; Hanafey, M. K.; Reilley, C. N. *J. Electroanal. Chem.* **1984**, *167*, 43, and references therein.
(16) Bange, K.; McIntyre, R.; Sass, J. K.; Richardson, N. V. *J. Electroanal. Chem.* **1984**, *178*, 351.
(17) Rudnick, J.; Stern, E. A. *Phys. Rev.* **1971**, *B4*, 4274.

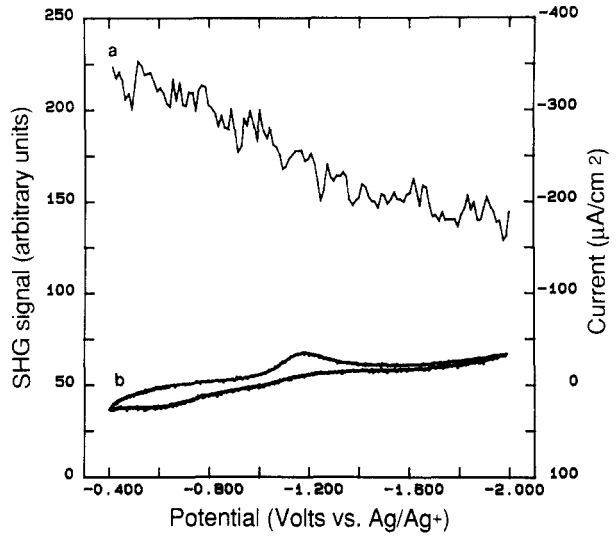

Figure 1. The average SHG signal (a) and the current (b) from a cyclic voltammogram as a function of potential at a polycrystalline silver electrode in a 0.1 M tetrabutylammonium tetrafluoroborate solution in acetonitrile. Scan rate: 10 mV s^{-1}. The SHG signal was independent of scan direction. The current peak at −1.18 V is due to the residual water.

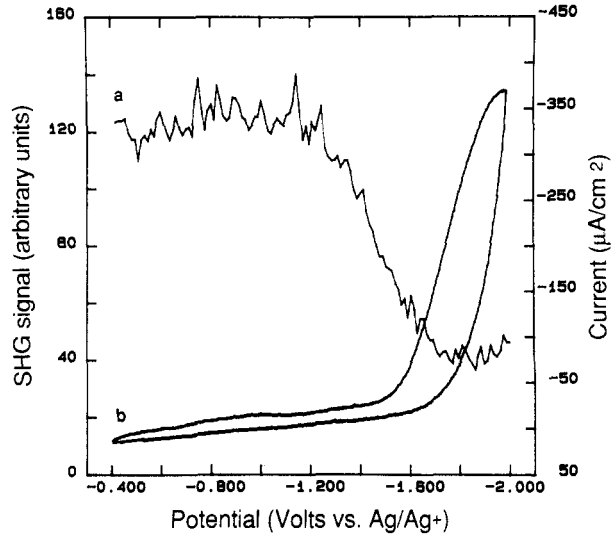

Figure 2. The SHG-potential curve (a) and cyclic voltammogram (b) at a polycrystalline silver electrode in a 0.1 M tetrabutylammonium tetrafluoroborate solution in acetonitrile containing 35 mM acetic acid. Scan rate: 10 mV s^{-1}.

at −1.18 V. However, no pronounced drop in SHG intensity such as that found in aqueous solutions[5] was observed. This is most likely due to the control of the surface properties by adsorbed acetonitrile molecules, which decrease the electric fields at the interface. This decrease also manifests itself in a decrease of the capacitance of the electrode; such effects have been reported in differential capacitance studies on gold and platinum electrodes in acetonitrile[13] (no differential capacitance studies have been reported on silver electrodes in acetonitrile). A decrease in the electric field strength at the surface suggests that, in agreement with our observations, the charge-induced SHG mechanism should not be as important in these solvents as in aqueous systems. The decrease in the SHG signal toward negative potentials in acetonitrile must be attributed *both* to the charge-induced SHG mechanism and to any changes in the adsorbed solvent layer due to the breakdown of the residual water.

In addition to the "reversible" (i.e., dependent only on the electrode potential) SHG signal, "irreversible" changes in the SHG signal were observed if the potential scans were extended in either direction. Irreversible changes in the optical signal were observed (1) at very negative potentials, due either to the reaction of lithium at the surface, to the cationic adsorption of tetrabutylammonium ions, or to the breakdown of the solvent; (2) at potentials more negative than −1.800 V after a very slight oxidation (<10 $\mu C/cm^2$) of the surface, in agreement with the findings of Richmond;[9] and (3) at more positive potentials (>−0.200 V) in the presence of any chloride or bromide impurities. A detailed analysis of these effects will be reserved for a later paper.

The cyclic voltammograms and averaged SHG-potential curves from acetonitrile solutions containing millimolar quantities of acetic, oxalic, and sulfuric acids are shown in Figures 2–4, respectively. In sulfuric acid a large (ca. 75%) irreversible loss in the SHG signal occurred during the first potential scan. The SHG signal from subsequent electrochemical scans was found to be independent of scan rate or direction, although reduced in magnitude. This irreversible loss during the first potential scan can be attributed to an acid-catalyzed surface reaction with either the solvent or the residual polishing alumina. To minimize this signal loss (and the possible concomitant passivation of the surface), all of the studies were performed with acid concentrations in the millimolar range. As one would expect, the least amount of difficulty was encountered with the weakest acid (i.e., acetic acid). In this concentration range, no hydrogen bubbles were observed on the electrode surface for any of these acid solutions.

Table I lists $E(i_p)$, the potential at which the maximum current due to hydrogen evolution is observed. This peak potential is

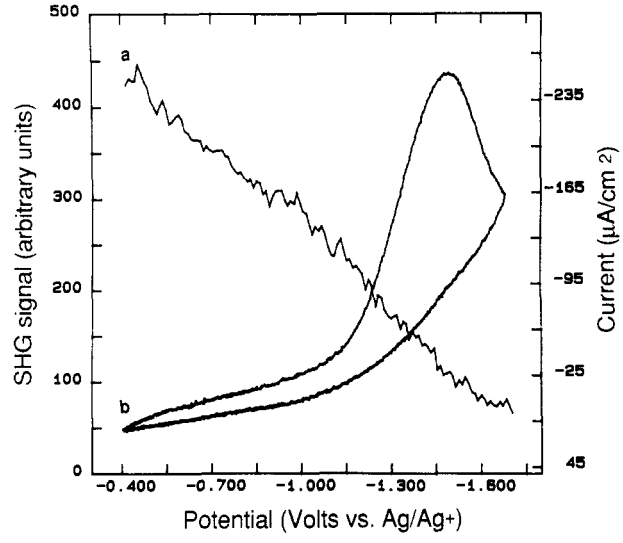

Figure 3. SHG-potential curve (a) and cyclic voltammogram (b) at a polycrystalline silver electrode in a 0.1 M tetrabutylammonium tetrafluoroborate solution in acetonitrile containing 20 mM oxalic acid. Scan rate: 10 mV s^{-1}.

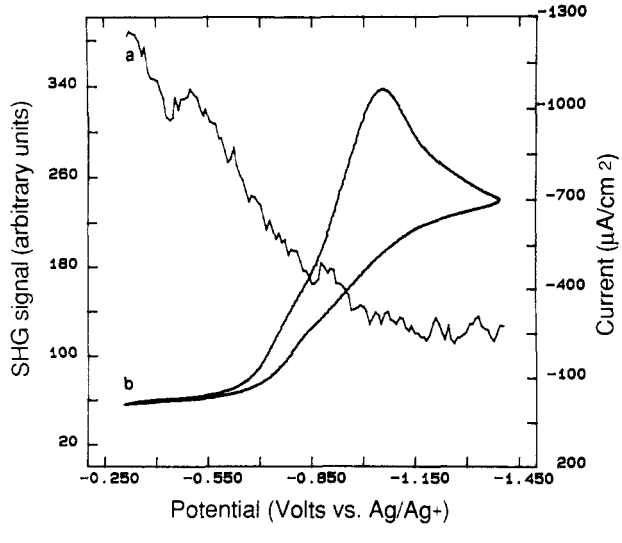

Figure 4. SHG-potential curve (a) and cyclic voltammogram (b) at a polycrystalline silver electrode in a 0.1 M lithium perchlorate solution in acetonitrile containing 5 mM sulfuric acid. Scan rate: 20 mV s^{-1}.

TABLE I: Potentials for the Peak Current, SHG Signal Diminution, and Formation of Adsorbed Hydrogen during the Hydrogen Evolution Reaction in Various Acidic Acetonitrile Solution[a]

acid	pK_a	pH	$E(i_p)$,[b] V	$E_{1/2}$(SHG), V	$E_{1/2}(\theta_r)$, V	$E_{1/2}(\theta_r)^{calcd}$, V
acetic	22.3	11.88	−1.98[c]	−1.45	−1.51	−1.50
oxalic	14.5[d]	8.40	−1.49	−1.08	−1.10	−1.12
sulfuric	7.25[d]	4.77	−1.05	−0.66	−0.72	−0.72
perchloric	e	2.30	−0.80	−0.38	−0.46	−0.45

[a] See text for a further explanation of the symbols. [b] An approximate potential as the current waveform is quite complex (see ref 17). [c] All potentials are V vs. Ag/Ag^+. [d] K_2 is neglected. [e] Completely dissociated.

approximate since the form of the hydrogen wave differs slightly for each acid solution. Listed along with the peak potentials in Table I is the pH (= −log a_{H^+} where a_{H^+} is the activity of the hydrogen ion species in acetonitrile) for each of the solutions studied as calculated from the literature values[18,19] for the acid dissociation constant, K_a (neglecting the second dissociation constant for oxalic and sulfuric acid). The peak potential changes systematically as a function of acid strength, in agreement with the results from Pt and Au electrodes,[20] and from classic polarographic studies.[21] The results from a millimolar solution of perchloric acid (which is completely dissociated in acetonitrile and which, like sulfuric acid, exhibited an irreversible SHG signal loss during the first electrochemical scan) are also included in the table.

In each of the Figures 2–4 it can be seen that there is a significant loss in the SHG signal prior to the observation of current from the evolution of molecular hydrogen at the electrode surface. The potential at which the SHG signal is halfway between its maximum and minimum value, $E_{1/2}$(SHG), is listed for the various acid solutions in Table I and has approximately the same pH dependence as the peak current potential. As with the cyclic voltammograms, the exact form of the SHG-potential curves varies slightly for each acid and is futher evidence of the changes in the reactivity of the polycrystalline silver surface as a function of acid strength.

Calculation of the Relative Surface Coverage of Adsorbed Hydrogen. The loss in SHG intensity must be attributed to some change in the electrode surface during the evolution of hydrogen. The possibility that the signal loss is due to the formation of microbubbles of molecular hydrogen at the surface is unlikely since (1) the SHG signal changes at a potential prior to that of the current wave in the cyclic voltammogram, and (2) SHG signal is stable at potentials where hydrogen is being evolved. The simplest interpretation is that the SHG is altered by the formation of a monatomic hydrogen intermediate on the electrode. The fact that the SHG signal is independent of scan rate and scan direction suggests that the amount of adsorbed hydrogen rapidly reaches some steady-state value at each potential. In acetonitrile, the amount of hydrogen adsorption during H_2 evolution is thought to be very small as compared to aqueous systems.[14] Although the SHG signal cannot give an absolute measure of the amount of surface coverage, the large changes that we observe suggest that on silver electrodes the coverages are at very least nonnegligible.

If we assume that the adsorbed hydrogen decreases the optical signal from the surface to an extent which is proportional to the relative surface coverage, $\theta/\theta_{max} = \theta_r$, then the nonlinear susceptibility must take the form

$$\chi^{(2)} = \chi_0^{(2)}(1 - c\theta_r) \quad (1)$$

where $\chi_0^{(2)}$ is the nonlinear susceptibility in the absence of adsorbed hydrogen, and c is a constant. Similar equations have been used to describe the change in SHG from a Rh surface in ultrahigh vacuum upon adsorption of CO or O_2.[22] The nonlinear susceptibility in eq 1 can be obtained from the SHG signal intensity, $I = |\chi^{(2)}|^2$, as a function of potential, and the constant c can be evaluated from the SHG signal at very negative potentials where we assume that $\theta_r = 1$. The experimentally determined relative surface coverages for acetic acid are plotted as a function of potential in Figure 5.

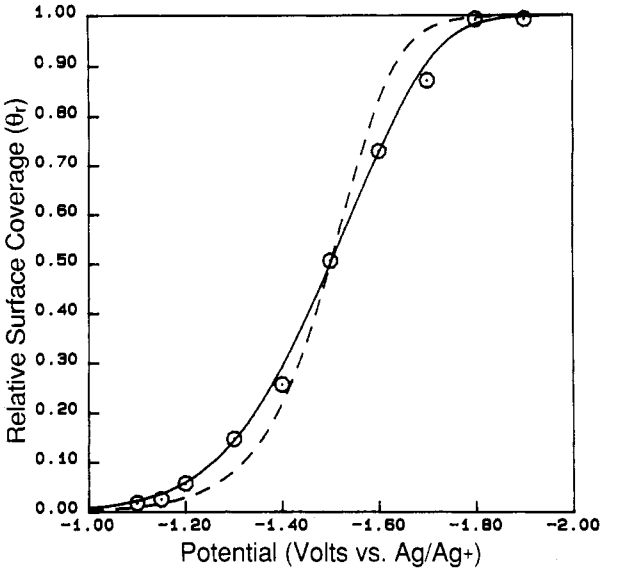

Figure 5. The relative surface coverage of adsorbed hydrogen as a function of electrode potential for acetic acid. The circles are calculated from the SHG signal by using eq 1, and the lines are the theoretical curves from eq 6 and 7 calculated by using the steady-state approximation with a surface combination reaction (reaction IIIb) as the final step: (---) $f = 0$, $E_0 = -0.100$ V, and $k_2/k_0 = 8.39$; (—) $f = 2.15$, $E_0 = -0.100$ V, and $k_2/k_0 = 1.60$.

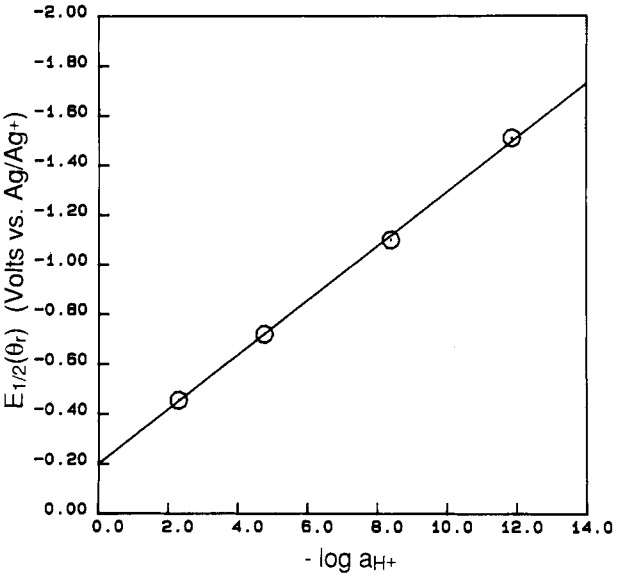

Figure 6. The potential, $E_{1/2}$, at which the relative surface coverage of adsorbed hydrogen (θ_r) calculated from the SHG data is equal to 0.5 plotted as a function of pH for the four acidic acetonitrile solutions studied. The straight line is the $E_{1/2}$–pH dependence predicted from the reaction mechanism for H_2 evolution by using eq 2.

Although the exact dependence of the relative surface coverage on electrode potential varies for each acid, we can find in each case the potential at which $\theta_r = 0.5$. These potentials are listed in Table I as $E_{1/2}(\theta_r)$ and plotted in Figure 6. As evident from the figure, $E_{1/2}$ is linearly related to the pH of the solution:

$$E_{1/2} = E_{1/2}^0 + \frac{RT}{\alpha F} \ln a_{H^+} \quad (2)$$

(18) Kolthoff, I. M.; Chantooni, M. K. *J. Am. Chem. Soc.* **1975**, *97*, 1376.
(19) Kolthoff, I. M.; Bruckenstein, S.; Chantooni, M. K. *J. Am. Chem. Soc.* **1961**, *83*, 3927.
(20) Sereno, E.; Macagno, V. A.; Giordano, M. C. *J. Electroanal. Chem.* **1977**, *76*, 199.
(21) Coetzee, J. F.; Kolthoff, I. M. *J. Am. Chem. Soc.* **1957**, *79*, 6110.
(22) Tom, H. W. K.; Mate, C. M.; Zhu, X. D.; Crowell, J. E.; Heinz, T. F.; Somorjai, G. A.; Shen, Y. R. *Phys. Rev. Lett.* **1984**, *52*, 348.

where α is a charge-transfer coefficient and $E_{1/2}{}^0$ is a constant. The slope and the intercept are determined from a least-squares fit to be −0.109 and −0.200 V, respectively; this slope corresponds to a value for α of 0.541. Any model of the hydrogen evolution reaction on silver electrodes must (1) be able to predict the experimental θ_r vs potential data in Figure 5, and (2) generate a $E_{1/2}$ vs pH curve that agrees with eq 2.

Determination of the Reaction Mechanism for Hydrogen Evolution. By comparing the potential and pH dependence of the relative surface coverage of adsorbed hydrogen from different models of the overall electrochemical process with that obtained from the SHG data, we can determine the reaction mechanism for H_2 evolution. In general, the H_2 evolution reaction in acidic media is thought to proceed through the following reaction mechanism:[23]

$$HA \overset{K_a}{\rightleftharpoons} H^+ + A^- \qquad (I)$$

$$H^+ + e \underset{k_{-1}}{\overset{k_1}{\rightleftharpoons}} H_{ad} \qquad (II)$$

$$H_{ad} + H^+ + e \xrightarrow{k_2'} H_2 \qquad (IIIa)$$

$$2H_{ad} \xrightarrow{k_2} H_2 \qquad (IIIb)$$

where k_2 is the rate constant for the surface combination reaction, and the rate constants k_1, k_{-1}, and k_2' all depend on the electrode potential in the standard fashion:

$$k_1 = k_0 \exp\left[-\frac{\alpha F}{RT}(E - E_0)\right] \exp(-\alpha f\theta) \qquad (3a)$$

$$k_{-1} = k_0 \exp\left[\frac{(1-\alpha)F}{RT}(E - E_0)\right] \exp((1-\alpha)f\theta) \qquad (3b)$$

$$k_2' = k_0' \exp\left[-\frac{\alpha' F}{RT}(E - E_0')\right] \exp(-\alpha' f\theta) \qquad (3c)$$

where α, E_0, and k_0 refer to reaction II, α', E_0', and k_0' refer to reaction IIIa, f is a constant which allows the free energy of adsorption to vary linearly with surface coverage (and will lead in the quasi-equilibrium approximation to a Frumkin isotherm),[23] and all the other symbols have their usual meaning. To simplify the equations we will assume that the coefficients α and α' are equal. We also neglect any effects due to adsorption of the acid HA or the anion A^- onto the electrode. Comparisons with our SHG results will show that with these assumptions we find that the hydrogen evolution reaction proceeds via reaction IIIb and not reaction IIIa, and that reaction II is an electrochemically irreversible process.

The relative values of the various rate constants in the reaction scheme above determine the surface coverage of adsorbed hydrogen on the electrode surface at a given potential. On some electrodes, such as platinum in aqueous acid solutions, the adsorption of hydrogen (reaction II) is a reversible equilibrium.[15] In these instances, the surface coverage of adsorbed hydrogen is appreciable and approaches a full monolayer. In other electrochemical systems, such as gold electrodes in aqueous acidic media, the adsorption process is irreversible and limits the steady-state coverage of adsorbed hydrogen to a small but finite value.[24]

These two different situations can be distinguished by the behavior of the faradaic current at potentials which correspond to the commencement of hydrogen evolution. A linear Tafel plot (log $|i|$ vs. E) for the hydrogen evolution reaction with a slope of $-\alpha F/2.3RT$ is indicative of either an electrochemically irreversible adsorption process, in which k_{-1} is zero, or a quasi-reversible adsorption process at a potential where k_{-1} is negligible. From the current observed in the acetic acid solution, we calculate a Tafel slope of approximately −9 V^{-1}. This value indicates that the adsorption process is electrochemically irreversible and yields a charge-transfer coefficient α that agrees with the value of 0.541 determined from the $E_{1/2}$ − pH plot in Figure 6. Such irreversible Tafel slopes have also been observed for the hydrogen evolution reaction on platinum and gold electrodes in acetonitrile.[20]

The electrochemically irreversible behavior of hydrogen adsorption on silver electrodes in acetonitrile is also verified by the inconsistencies that we observe when we attempt to compare the relative surface coverages calculated from the SHG data to coverages obtained from model calculations which assume a *reversible* adsorption process. If reaction II is in equilibrium, then θ_r can be calculated from a Langmuir or Frumkin adsorption isotherm.[23] We find that we are unable to fit the experimental $\theta_r - E$ plot for acetic acid in Figure 5 with a Langmuir adsorption isotherm. The addition of the constant f in the rate constants for reaction II (eq 3a and 3b) leads to a Frumkin adsorption isotherm which approximately fits the data. However, *both* the Langmuir and Frumkin adsorption isotherms incorrectly predict the $E_{1/2}$ dependence on ln a_{H^+} (eq 2), yielding a slope of RT/F instead of the observed $RT/\alpha F$. For this reason, as well as the irreversibility exhibited in the Tafel and $E_{1/2}$ − pH plots, both the Langmuir and Frumkin isotherms in this quasi-equilibrium approximation must be rejected.

Thus we find that the H_2 evolution reaction commences with an electrochemically irreversible (or at best quasi-reversible) adsorption of monatomic hydrogen. By assuming that the formation of molecular hydrogen proceeds via reaction IIIa or IIIb, a theoretical θ_r vs. potential curve can be calculated from the steady-state solution of the reaction mechanism. We also assume that the hydrogen ion activity in solution remains constant throughout the scan (no depletion layer is generated assuming that reaction I is very fast). The exact form of the relation of $\theta_r(E)$ depends upon whether k_{-1} is zero (totally irreversible adsorption) or just very small (quasi-reversible adsorption). Examination of the $\theta_r(E)$ curves for the two possible reaction mechanisms shows that, with either an irreversible or quasi-reversible adsorption process, the experimental data can be fit only by assuming that H_2 is formed by the surface combination reaction IIIb:

(1) Steady-State Assumption with Reaction IIIa. If we assume that H_2 is forrmd by a second ion-discharge reaction (reaction IIIa), then θ_r in the steady-state approximation is independent of electrode potential if reaction II is totally irreversible and has a potential dependence given by eq 4 if reaction II is quasi-reversible:

$$\theta_r = \frac{1 + b}{1 + b + a_{H^+}{}^{-1} \exp\left[\frac{F}{RT}(E - E_0)\right] \exp(f\theta_r)} \qquad (4)$$

where the parameter b is a constant:

$$b = \frac{k_0'}{k_0} \exp\left[\frac{\alpha F}{RT}(E_0' - E_0)\right] \qquad (5)$$

The behavior predicted by the irreversible case is obviously incorrect. With the quasi-reversible steady-state solution (eq 4 and 5), we obtain results that are similar to the Langmuir and Frumkin adsorption isotherms in the quasi-equilibrium case. The $\theta_r(E)$ curves in Figure 5 for acetic acid can be approximately fit only if we let f be nonzero, but once again the predicted $E_{1/2}$ − ln a_{H^+} dependence (eq 2) has the incorrect slope of RT/F. Therefore, we must rule out the possibility that the hydrogen evolution reaction proceeds via reaction IIIa.

(2) Steady-State Assumption with Reaction IIIb. If we assume that a surface combination reaction (reaction IIIb) is the final step in the H_2 evolution reaction, then the potential dependence of θ_r in the steady-state approximation is given by eq 6a if reaction II is quasi-reversible:

$$\theta_r = \frac{1}{1 + b + a_{H^+}{}^{-1} \exp\left[\frac{F}{RT}(E - E_0)\right] \exp(f\theta_r)} \qquad (6a)$$

(23) Gileadi, E.; Conway, B. E. *J. Chem. Phys.* **1963**, *39*, 3420.
(24) Kuhn, A. T.; Byrne, M. *Electrochim. Acta* **1971**, *16*, 391.

and by eq 6b if the adsorption process is totally irreversible:

$$\theta_r = \frac{1}{1+b} \tag{6b}$$

where the parameter b is a function of θ_r and E:

$$b = \frac{2k_2\theta_r}{k_0 a_{H^+}} \exp\left[\frac{\alpha F}{RT}(E - E_0)\right] \exp((1+\alpha)f\theta_r) \tag{7}$$

Using numerical analysis, we can solve eq 6 and 7 and generate theoretical $\theta_r - E$ curves which fit the experimental data; virtually identical curves are obtained in the irreversible and quasi-reversible cases. Plotted in Figure 5 are examples of the type of fits we obtain when $f = 0$ (dashed line) and $f = 2.15$ (solid line). A range of values for E_0 and k_2/k_0 could be found which yielded acceptable $\theta_r - E$ curves, but the two constants were interrelated. This relation can be explained by examining the $E_{1/2} - \ln a_{H^+}$ dependence. We can derive eq 2 with the *correct* slope of $RT/\alpha F$ from eq 6a by assuming that

$$\exp\left[\frac{(1-\alpha)F}{RT}(E_{1/2} - E_0)\right] \ll \frac{k_2}{k_0}\exp(\alpha f/2) \tag{8}$$

where $E_{1/2}$ is the potential at which $\theta_r = 0.5$. $E_{1/2}$ is then proportional to $(RT/\alpha F) \ln a_{H^+}$ as in eq 2, and the intercept $E_{1/2}{}^0$ is given by

$$E_{1/2}{}^0 = E_0 - \frac{RT}{\alpha F}\ln\frac{k_2}{k_0} - \frac{(1+\alpha)RT}{2\alpha F}f \tag{9}$$

With an intercept determined from the values of α, E_0, f, and k_2/k_0 used in generating the θ_r–E curves for acetic acid in Figure 5, the $E_{1/2}$ values for the various acid solutions are calculated and listed in Table I as $E_{1/2}(\theta_r)^{calcd}$. The agreement is excellent. In principle, the best possible combination of the three parameters E_0, f, and k_2/k_0 could be determined by an accurate measurement of θ_r for all of the acids studied, but this was not attempted with our data. Nevertheless, since this reaction mechanism correctly predicts a slope of $RT/\alpha F$ for eq 2, we conclude that the hydrogen evolution reaction proceeds on silver electrodes in acetonitrile via the nonreversible adsorption of monatomic hydrogen onto the surface followed by a surface combination reaction to produce molecular hydrogen.

Conclusions

In summary, our studies here indicate conclusively that the SHG from polycrystalline silver electrodes in acidic acetonitrile solutions shows a "reversible" decrease with changes in the applied potential during the evolution of molecular hydrogen. This decrease is attributed to a modification of the optical properties of the metal surface by the formation of an adsorbed monatomic hydrogen species. One explanation for this effect is that the adsorbed hydrogen is engaging or scattering free electrons at the surface which would otherwise contribute to the nonlinear susceptibility. Another interpretation of the loss in signal is that the H_2 evolution reaction discharges the excess charge density on the electrode, and that this decrease leads to a change in the optical signal via the charge-induced SHG mechanism. In the absence of H_2 evolution, changes in the SHG signal as a function of potential are found to be smaller in acetonitrile than in aqueous solutions due to the effects of solvent adsorption on the electric fields at the interface.

By comparing the potential and pH dependence of the relative surface coverage of adsorbed hydrogen that we calculate from our SHG measurements with that predicted from various reaction mechanisms, we conclude that the H_2 evolution reaction on silver electrodes in acetonitrile solutions occurs via a two-step process. An irreversible or quasi-reversible electrochemical charge-transfer reaction creates a monatomic hydrogen species on the electrode surface and is followed rapidly by a biatomic surface combination reaction to form molecular hydrogen. Our studies on the H_2 evolution reaction demonstrate that SHG can be a valuable tool in monitoring adsorbed surface intermediates during an electrochemical process. In the future we plan to extend our SHG studies to other metal and semiconductor electrodes,[25] and to cases where molecular adsorption directly contributes to the SHG intensity.[26-28]

Acknowledgment. The authors thank Profs. D. Evans, D. Buttry, and M. J. Weaver for very helpful discussions, and Prof. T. Furtak for a preprint of his paper. This work was supported in part by grants from Research Corporation and the Wisconsin Alumni Research Foundation.

Registry No. H_2, 1333-74-0; Ag, 7440-22-4; acetic acid, 64-19-7; oxalic acid, 144-62-7; sulfuric acid, 7664-93-9; perchloric acid, 7601-90-3.

(25) Lee, C. H.; Chang, R. K.; Bloembergen, N. *Phys. Rev. Lett.* **1967**, *18*, 167.
(26) Heinz, T. F.; Tom, H. W. K.; Shen, Y. R. *Phys. Rev.* **1983**, *A28*, 1883.
(27) Van Wyck, N. E.; Koenig, E. W.; Byers, J. D.; Hetherington III, W. M. *Chem. Phys. Lett.* **1985**, *122*, 153.
(28) Hicks, J. M.; Kemnitz, K.; Eisenthal, K. B.; Heinz, T. F. *J. Phys. Chem.* **1986**, *90*, 560.